Cellular Physiology and Biochemistry

Cell Physiol Biochem 2018;45:429-445
DOI: 10.1159/000486920
Published online: January 29, 2018
Accepted: December 10, 2017

Original Paper

Key Proteins Involved in Spheroid Formation and Angiogenesis in Endothelial Cells After Long-Term Exposure to Simulated Microgravity

Anita Dittrich[a,b] Daniela Grimm[a,c,d] Jayashree Sahana[a] Johann Bauer[e] Marcus Krüger[c,d] Manfred Infanger[d] Nils E. Magnusson[b]

[a]Institute of Biomedicine, Pharmacology, Aarhus University, Aarhus C, [b]Medical Research Laboratory, Department of Clinical Medicine, Aarhus University, Aarhus C, Denmark; [c]Gravitational Biology and Translational Regenerative Medicine, Otto-von-Guericke-University Magdeburg, Magdeburg, [d]Clinic for Plastic, Aesthetic and Hand Surgery, Otto-von-Guericke-University Magdeburg, Magdeburg, [e]Max-Planck-Institute of Biochemistry, Martinsried, Germany

Key Words
Microgravity • Endothelial cells • Angiogenesis • Endothelial dysfunction • Multicellular spheroids • Tube formation • Random Positioning Machine

Abstract
Background/Aims: Cardiovascular complications are common in astronauts returning from a prolonged spaceflight. These health problems might be driven by complex modulations of gene expression and protein synthesis in endothelial cells (ECs). Studies on the influence of microgravity on phenotype, growth pattern and biological processes of ECs can help to understand these complications. ***Methods:*** We exposed ECs (EA.hy926) to a Random Positioning Machine (RPM). Proteins associated with cell structure, angiogenesis and endothelial dysfunction were investigated in distinct pools of multicellular spheroids (MCS), adherent cells (AD) and tubular structures (TS) formed after a 35-day RPM-exposure. ***Results:*** Combining morphological and molecular approaches, we found AD, MCS and TS with changes in the synthesis and release of proteins involved in three-dimensional growth. Fibronectin and monocyte chemoattractant protein-1 (MCP-1) mRNAs and protein contents were elevated along with an increased secretion of vascular endothelial growth factor (VEGF), interleukin (IL)-6, IL-8, MCP-1, intercellular adhesion molecule 1 (ICAM-1), vascular cell adhesion molecule 1 (VCAM-1), neutrophil gelatinase-associated lipocalin (NGAL) and regulated on activation, normal T cell expressed and secreted (RANTES) proteins in the culture supernatant as determined by multianalyte profiling technology. Together they form a network of interaction. ***Conclusions:*** These results show that a prolonged RPM-exposure of ECs induced TS and MCS formation. The factors VEGF, NGAL, IL-6, IL-8, MCP-1, VCAM-1, ICAM-1, fibronectin and RANTES seem to be affected when gravity is omitted.

Daniela Grimm

Gravitational Biology and Translational Regenerative Medicine,
Otto-von-Guericke-University Magdeburg, Zenit, Building 65, Magdeburg (Germany)
Tel. +45-871 67693, Fax +45-8612-8804, E-Mail dgg@biomed.au.dk

Introduction

The impact of microgravity on different cell types is currently a topic of interest. Astronauts suffer of various health problems after a long-term space travel. Cardiovascular problems like hypotension and arrhythmias might occur. A recent study showed that a dysfunctional vestibular system induces a blood pressure drop in astronauts returning from a space mission [1]. Endothelial cells (ECs) play a key role in the pathogenesis of various diseases and are highly sensitive to microgravity. ECs were investigated in space on the International Space Station (ISS) [2, 3] and on Earth using techniques to simulate microgravity [4-7]. With the help of so-called ground-based facilities like clinostats or the RPM, which are devices constructed to simulate microgravity, some aspects of annulling gravity can be studied. Such devices trigger at least a part of the incubated cells to detach from the bottom of a culture flask and to form 3D aggregates like they are observed after spaceflights [2]. ECs have shown that they grow as three-dimensional (3D) aggregates in form of multicellular spheroids (MCS) or tubular structures (TS) without any scaffold when they were exposed to the RPM or had been cultured in space on the ISS [2, 8]. The morphology of these aggregates had been investigated earlier [8]. The TS exhibited a lumen and the walls consist of a single layer of ECs resembling a vascular intima. The process of tube formation started between the 5th and 7th day [9]. The cells had arranged themselves in line and formed a tube from accumulated extracellular matrix (ECM) proteins [8]. The mechanisms for this behavior are still not completely clear. A recent study showed that ras homolog gene family member A (RhoA) inactivation supports the actin rearrangement-associated angiogenic responses in human umbilical vein endothelial cells (HUVECs) during simulated microgravity [7]. Early cytoskeletal changes of microgravity-exposed ECs have previously been described in real and simulated microgravity [10, 11].

There is evidence of a direct correlation of the cytoskeletal changes upon microgravity and transcription alterations [12]. It is suggested that the interaction of the extracellular matrix (ECM), cell adhesion and connection to cytoskeleton are the basis of gravisensing in human cells [12].

In this study, we focused on long-term changes of ECs exposed to a RPM for 35 days and investigated proteins known to be involved in the process of angiogenesis as well as factors secreted into the culture supernatant. The relationship of factors driving the 3D growth of ECs in a microgravity-dependent system such as vascular endothelial growth factor (VEGF) and its receptors fetal liver kinase 1 (Flk1 or kinase insert domain receptor (KDR) or VEGFR-2) and Fms-related tyrosine kinase 1 (Flt1 or VEGFR-1), cytokines like the interleukins (IL)-6 and IL-8, plasminogen activator inhibitor 1 (PAI-1), monocyte chemoattractant protein 1 (MCP-1 or CCL2), the cell adhesion molecules vascular cell adhesion molecule 1 (VCAM-1) and intercellular adhesion molecule 1 (ICAM-1) were investigated.

In addition, we focused on ECM proteins and on inflammation factors released in the culture supernatant by the ECs.

The principal aim of these investigations was to find further reasons why simulated microgravity conditions are associated with a change in growth behavior and increased spheroid and tube formation (angiogenesis) of these ECs.

The results obtained suggested that the 3D growth of ECs in a microgravity-dependent system is driven via a network of genes and proteins involved in cell structure maintenance and intercellular signaling.

Materials and Methods

Cell culture

The permanent human cell line EA.hy926 expresses factor VIII-related antigen a marker of vascular endothelial function [13].

The cell line had been established by fusing HUVEC with the permanent cell line A549, which derived from a human lung carcinoma. EA.hy926 cells were grown in RPMI 1640 medium (Invitrogen, Eggenstein,

Germany) supplemented with 10% fetal bovine serum (Biochrom, Berlin, Germany), 100 units/mL penicillin and 100 µg/mL streptomycin (Invitrogen).

The cells were grown in 75-cm^2 culture flasks (Sarstedt, Nümbrecht, Germany) until subconfluent monolayers were formed. After reaching a subconfluency of 80%, the cells were subcultured into T-25 cell culture flasks (10^6 cells/flask). The next day the adherent monolayers were randomized into the following study groups: 35-day (d) 1*g*-group and 35-d RPM-group. T-25 cell culture flasks at 1*g* were subcultured and collected at days 7, 14, 21, 29 and 35. The flasks were filled completely with medium, to avoid air bubbles and were either mounted on the RPM (Fig. 1A), a device created to realize microgravity conditions on Earth (Airbus, Defense and Space, Leiden, the Netherlands), or kept in the same incubator next to the RPM at 1*g* with a constant temperature of 37 °C and 5% CO_2. The general behavior of cells on the RPM had been thoroughly investigated and previously published in detail [11, 14-19].

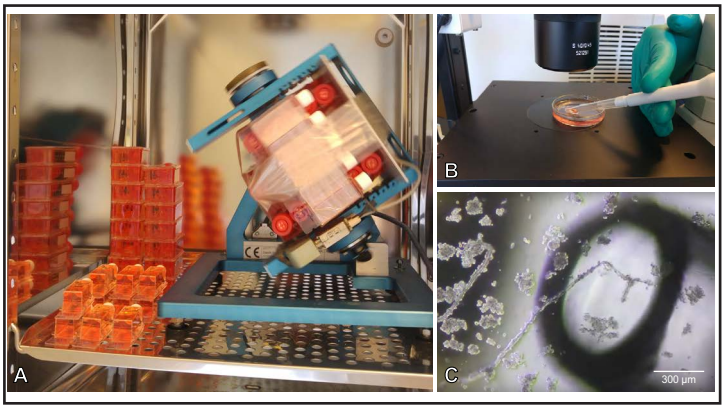

Fig. 1. Procedure of the experiments: Cultures of EA.hy926 cells on the RPM and collection of MCS and tubular structures. T-25 flasks and slideflasks are placed in the incubator under 1*g*-conditions or secured on the RPM (A), here seen while in motion. Collecting TS using a 1 mL pipette tip (B). TS collected with a pipette under the phase contrast microscope at day 35 (C).

Cells of T-25 cell culture flasks at the RPM were collected at day 35 (n=15) and used for Western blot analyses and quantitative PCR (qPCR). Adherently growing cells from the 1*g*- and µ*g* (microgravity)-conditions were collected by scraping off the cells from the bottom of the culture flasks in 5 mL ice-cold phosphate buffered saline (PBS). The MCS from the µ*g*-samples were collected by centrifugation (4°C) of the supernatants and followed by washing with PBS. TS were collected with a pipette under microscopy (Fig. 1B, C). They were pooled from 15 flasks for qPCR by transferring portions of the supernatant to a petri dish, using a standard pipette with a 1 mL tip to extract the TS under a phase contrast microscope (Fig. 1C). Dry pellets from all T25 samples were snap frozen in liquid nitrogen and kept at -80°C while the TS were preserved in TRIzol® reagent (Thermo Fischer Scientific, Waltham, MA USA) and kept at -20°C.

Slide flasks kept at 1*g* (n=20) and µ*g* (n=20) were all collected at day 35 and used directly for immunofluorescence staining. Every three days, starting at day 5 one third of the medium was replaced with fresh medium and the cells examined by phase contrast microscopy (Leica Microsystems GmbH, Wetzlar, Germany) and photographed using a Canon EOS 550D. Supernatant samples were collected from T-25 flasks, centrifuged at 4°C and kept at -20°C.

Immunofluorescence staining

Slideflasks were kept intact while the cells were fixed using a 4% paraformaldehyde solution for 20 min, then subjected to membrane permeabilization with ice-cold methanol for 10 min and blocking with 1% bovine serum albumin (BSA, Sigma-Aldrich, Steinheim, Germany) in PBS for 15 min. The slides were then released from the flasks and the cells incubated with primary antibodies in a PBS solution with 1% BSA for 24 h at room temperature (RT), followed by washing and incubation with secondary antibodies in PBS solution with 1% BSA for an additional 24 h. The used antibodies for these investigations are given in Table 1. The cells were washed and prepared for microscopy using Fluoroshield™ mounting media with DAPI (4',6-diamidino-2-phenylindole; Sigma-Aldrich-F6057). Slides were kept at 4°C in a dark box for 2 days before confocal laser scanning microscopy. The stained samples were examined using a Zeiss 510 META inverted confocal laser scanning microscope (Zeiss, Germany), equipped with a Plan-Apochromat 63×1.4 objective [20]. Excitation and emission wavelengths were: λ_{exc} = 488 nm and λ_{em} ≥505 nm for FITC. Afterwards, the samples were analyzed with the help of the image analysis program Scion Image (Version 1.63 MacOs, Scion Corporation, USA).

Western blot analyses

The method for Western blotting was published earlier in detail [21-23]. Cell pellets solubilized in lysis buffer were measured for total protein concentration using Bio-Rad DC™ protein assay (BioRad, USA), and samples for Western blot prepared accordingly with Laemmeli buffer with 5% β-mercaptoethanol for a final protein concentration of 2 µg/µL. Samples were denatured at 95°C for 15 min. 15 µL of each sample was loaded on TGX Stain-free precast gels and electrophoresis performed in Criterion electrophoresis chambers (BioRad). Gels were transferred to membranes (Trans-Blot Turbo™ PVDF membrane pack) using the Trans-Blot turbo transfer system (BioRad). Blocking of the membrane was done in 0.3% I-block in PBS (Applied Biosystems, USA) for 3 h at RT. The membranes were incubated with primary and secondary antibody solutions (PBS with 1% BSA) for 24 h and 2 h respectively. Super Signal™ West kit (Thermo Fisher) was used to develop the membranes for imaging with the ChemiDoc system (Bio-Rad). Total protein images of the gels were also taken with the ChemiDoc and used for normalization. A complete list of antibodies used in this study is shown in Table 1.

Table 1. Antibodies used for western blot analyses and immunofluorescence**.** AB, antibody; n.d. not done; sigma, Sigma Aldrich, HAF007, HAF008 are both from R&D systems; Sc, Santa Cruz Biotechnology, Mabn, Merck Millipore; Ab, Abcam; AF488, Alexa Fluor®488 Thermo Fisher Scientific; RHO, rhodamine conjugate, Thermo Fisher Scientific

Target protein	Western blot			Immunofluorescence		
	Primary AB	Dilution	Secondary AB	Primary AB	dilution	Secondary AB
Fibronectin	sigmaF3648	1:1000	HAF008	sigmaF3648	1:150	Goat anti-Rabbit IgG (H+L) AF488
VEGF	Sc7269	1:1000	HAF008	Ab46151	1:150	Goat anti-mouse IgG (H+L) RHO
MCP-1	Mabn712	1:500	HAF007	Mabn712	1:250	Goat anti-Mouse IgG (H+L) AF488
TGF-β	Ab92486	1:250	HAF008	Ab92486	1:250	Goat anti-rabbit IgG (H+L) AF488
PAI-1	Ab66705	1:500	HAF008	Ab66705	1:500	Goat anti-rabbit IgG (H+L) AF488
IL-6	n.d.			Sc28343	1:50	Goat anti-mouse IgG (H+L) RHO
IL-8	n.d.			Sc7922	1:50	Goat anti-rabbit IgG (H+L) AF488
NGAL	n.d.			Sc50350	1:50	Goat anti-rabbit IgG (H+L) AF488

Neutrophil gelatinase-associated lipocalin (NGAL) and VEGF 165 measurements

A time resolved immunofluorometric assay (TRIFMA) was used to measure the levels of NGAL (LCN2) and VEGF 165 in the supernatants collected at the days 5, 14, 23, 29 and 35 following previously described methods [24-26].

Cytokine measurements by multianalyte profiling (MAP) technology

The different cytokines and proteins released into the supernatants of the cell cultures, were analyzed by the company Myriad RBM (Austin, Texas, USA). The MAP analysis was performed using the Human Inflammation kit® as described previously [24]. Supernatants were taken after 35 d from 1*g*- (n = 5) and RPM-samples (n = 13) and stored at -80°C until shipment to Myriad RBM.

RNA isolation and quantitative real-time PCR

The RNA isolation and quantitative real-time PCR (qPCR) were performed as described earlier in detail [2, 25, 27]. RNA and proteins were isolated using the AllPrep RNA/Protein kit (Qiagen GmbH, Hilden, Germany) according to the manufacturer's recommendations. The RNA was determined with the SpectraMax M2 (Molecular Devices, California, USA). Reverse transcription was done using the First Strand cDNA Synthesis Kit (Thermo Scientific, Waltham, Massachusetts, USA) according to the manufacturer's protocol. With the qPCR we determined the expression levels of target genes listed in Table 2, using the SYBR® Select Master Mix (Applied Biosystems, Darmstadt, Germany) and the 7500 Real-Time PCR System (Applied Biosystems). cDNA-selective primers were designed to span exon-exon boundaries and to have a T_m of 60 °C using Primer Express software (Applied Biosystems), and were synthesized by TIB Molbiol (Berlin, Germany). All samples were measured in triplicate and normalized to the housekeeper 18S rRNA. Comparative CT (ΔΔCT) methods were used for relative quantification of transcription levels, with 1*g* set as 100%.

STRING Analysis

Interactions between proteins were determined using the STRING 10 platform [28]. For each protein, the UniProtKB entry number was inserted in the input form "multiple proteins" and "Homo sapiens" was

selected as organism. The resulting network view was downloaded in the molecular action view showing lines between interacting proteins and genes [29].

Statistical Evaluation

Statistical Evaluation was performed using SPSS 15.0 (SPSS, Inc., Chicago, IL, USA). The Mann-Whitney-U-Test (protein release) or a Student's *t*-tests (gene expression) were used to compare 1*g* and s-µ*g* conditions, as well as AD cells and MCS cells. All data is presented as mean ± standard deviation (SD) with a significance level of $p < 0.05$.

Table 2. Primers used for quantitative real-time PCR

Gene	Primer	Sequences (5'-3' direction)
CCL2	MCP1-F	GCTATAGAAGAATCACCAGCAGCAA
	MCP1-R	TGGAATCCTGAACCCACTTCTG
COL4A1	COL4A1-F	AAAGGGAGATCAAGGGATAG
	COL4A1-R	TCACCTTTTTCTCCAGGTAG
CXCL8	IL8-F	TGGCAGCCTTCCTGATTTCT
	IL8-R	GGGTGGAAAGGTTTGGAGTATG
FLK1	FLK1-F	TCTTCTGGCTACTTCTTGTCATCATC
	FLK1-R	GATGGACAAGTAGCCTGTCTTCAGT
FLT1	FLT1-F	CCCTCGCCGGAAGTTGTAT
	FLT1-R	GATAATTAACGAGTAGCCACGAGTCAA
FN1	FN1-F	TATGAGCAGGACCAGAAATAC
	FN1-R	CCACTTCATGTTGTCTCTTC
IL6	IL6-F	CGGGAACGAAAGAGAAGCTCTA
	IL6-R	GAGCAGCCCCAGGGAGAA
SERPINE1	PAI1-F	AGGCTGACTTCACGAGTCTTTCA
	PAI1-R	CACTCTCGTTCACCTCGATCTTC
TGFB1	TGFB1-F	CACCCGCGTGCTAATGGT
	TGFB1-R	AGAGCAACACGGGTTCAGGTA
VEGFA	VEGF-F	AATGTGAATGCAGACCAAAG
	VEGF-R	GACTTATACCGGGATTTCTTG
YWHAQ (housekeeper)	YWHAQ-F	GGTACCTTGCTGAAGTTGCG
	YWHAQ-R	GGGTGTGTGGGTTGCATCT

Results

Three phenotypes of endothelial cells after RPM-exposure

We had recently shown that after five and seven days in space and on the RPM, adherently growing cells (AD), multicellular spheroids (MCS) and small tubular structures (TS) can be observed [2, 8, 9, 15]. In 1*g*-cultures no 3D aggregates were detectable. The timeline of 3D aggregation was shown in previous experiments [8, 9, 15]. In this paper, we focused on 35-d spheroids and TS (Fig. 2A-C). At day 35 large numbers of TS could be collected. On average, each T-25 flask contained 12-15 TS with a length of approx. 500-800 µm and 3-5 larger TS with a length of about 2-3 mm, which could be seen with the naked eye in a petri dish (Fig. 1C). The TS were investigated by qPCR, and the MCS by qPCR, Western blotting, and immunofluorescence. The cell culture supernatants were measured by MAP technology.

Extracellular matrix proteins

For immunofluorescence staining (IFS) three groups of samples (1*g*, RPM-AD and RPM-MCS) were used and collected at day 35 (Fig. 3A).

Visualization of fibronectin protein by IFS revealed a decrease in AD cells and an elevated accumulation in the MCS cells at day 35 compared to the 1*g*-control cells (Fig. 3A). This result is supported by the gene expression of *FN1* determined by qPCR (Fig. 3B) and confirmed by Western blot analysis (Fig. 3F).

Moreover, we investigated transforming growth factor-beta1 (TGFB1) by IFS (Fig. 3D). Although a slightly more intensive staining of TGFB1 in ECs exposed to the RPM appeared, Western blotting did not reveal any

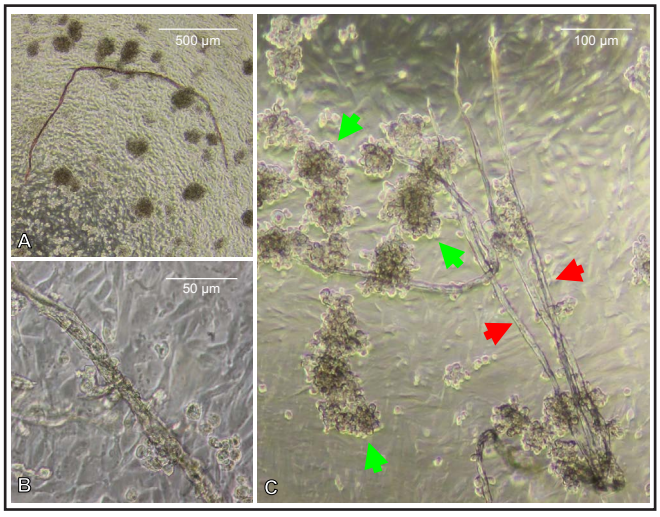

Fig. 2. Morphologic examination of the cells: Phase-contrast microscopy of EA.hy926 cells exposed to the RPM for 35 days. Samples cultured for 35 d on the RPM (A, B) revealed cells that stayed adherently as a monolayer (AD), MCS and large TS. Detailed view of TS and MCS on day 35 (C). Green arrowheads show MCS and red arrowheads mark TS.

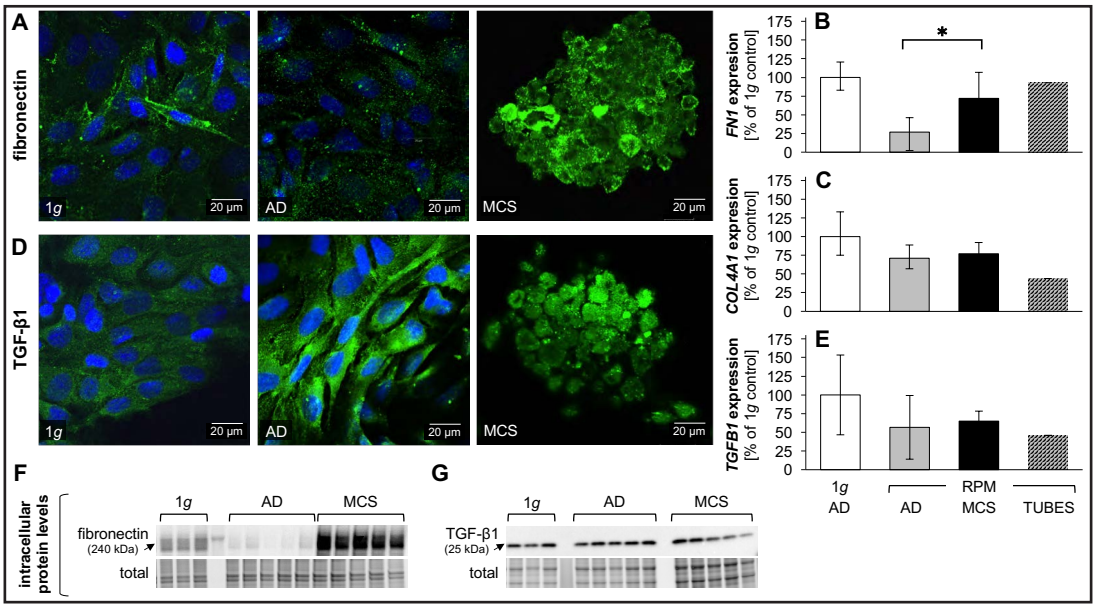

Fig. 3. Influence of RPM-exposure on the extracellular matrix of ECs: Quantitative alterations of protein content and gene expression of ECM-associated proteins after 35 d. Fibronectin. Immunofluorescence images of 1*g*-control cells, RPM-AD and RPM-MCS (A), Expression of *FN1* (B). Collagen-IV. Expression of *COL4A1* (C). TGF-β_1. Immunofluorescence images of 1*g*-control cells, RPM-AD and RPM-MCS (D). Expression of *TGFB1* (E). Intracellular levels of fibronectin (F) and TGF-β_1 determined via Western Blot (G). *p<0.05. Scale bars: 20 µm.

changes in the cellular protein content (Fig. 3G). In addition, the *TGFB1* gene expression was not altered in all groups (Fig. 3E). A similar result was detected for the mRNA expression of *COL4A1* (Fig. 3C).

Regulation of Vascular Endothelial Growth Factor in ECs exposed to the RPM

VEGF is an important regulator of angiogenesis and tube formation [11, 30]. We focused on the gene expression of *VEGFA*, on the VEGF protein level and the secretion of VEGF165 in the cell culture supernatant. This data is given in Fig. 4.

IFS of VEGF revealed that the amount of VEGF protein is subtly increased in the AD samples and more pronounced in the RPM-MCS cells compared to the 1*g*-controls (Fig. 4A). Interestingly, the qPCR data revealed that *VEGFA* is not differentially regulated (Fig. 4B).

Soluble VEGF protein was measured in the cell supernatants at different time points (5 d, 14 d, 23 d, 29 d and 35 d) (Fig. 4C). The concentration of secreted VEGF was significantly increased at day 35 and all other time points in µ*g*-supernatants.

In addition, we measured the gene expression of *FLT1* and *FLK1* (Fig. 4D, E). The mRNAs of both VEGF receptors were not significantly changed in all groups.

The cytokines interleukin-6 and interleukin-8 in spheroid formation

IFS revealed an accumulation of interleukin-6 (IL-6) in spheroids as compared to AD cells and 1*g* cells (Fig. 5A). There was a tendency of an increase in *IL6* mRNA in spheroids and tubes compared to 1*g*-samples (Fig. 5B). In addition, the release of IL-6 protein in the supernatant was significantly elevated in RPM-samples (Fig. 5E).

Interleukin-8 (IL-8) plays an important role in 3D growth and spheroid formation of cancer cells and benign cells [20, 31, 32]. Therefore, we focused on IL-8 in these experiments. IFS visualized a clear accumulation of IL-8 protein in the spheroids compared to AD and 1*g*-cells (Fig. 5C). These results were supported by the upregulated *CXCL8* mRNA level in the MCS group as compared to all other groups (Fig. 5D). Moreover, the secretion of IL-8 protein, as measured by MAP technology, was significantly enhanced in RPM-samples (Fig. 5E).

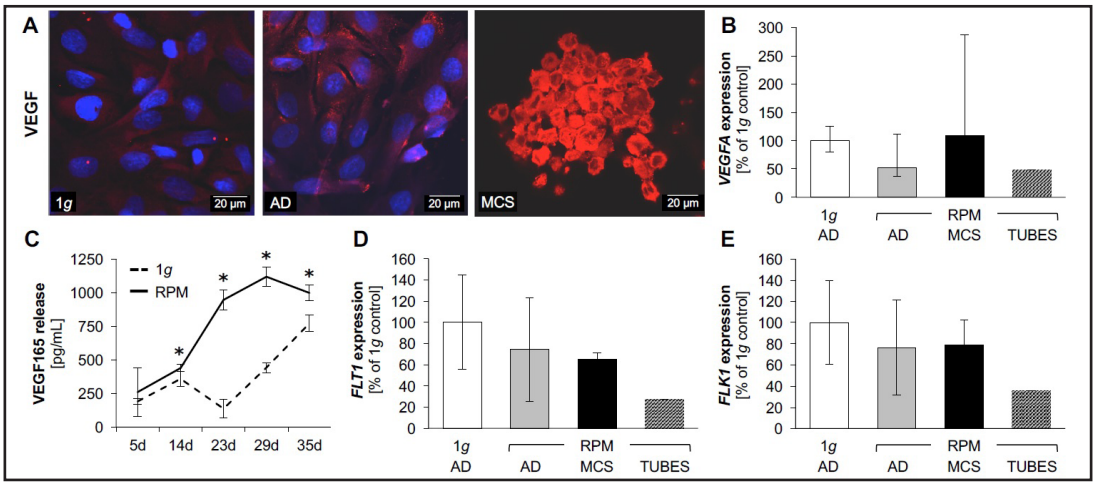

Fig. 4. Influence of RPM-exposure on Vascular Endothelial Growth Factor. Quantitative alterations of protein content and gene expression of VEGF and VEGF receptors after 35 d. VEGF. Immunofluorescence images of 1*g*-control cells, RPM-AD and RPM-MCS (A). Expression of *VEGFA* (B). Time course of VEGF165 release by the ECs (C). VEGF receptors. Expression of *FLT1* (D) und *FLK1* (E). *p<0.05. Scale bars: 20 µm.

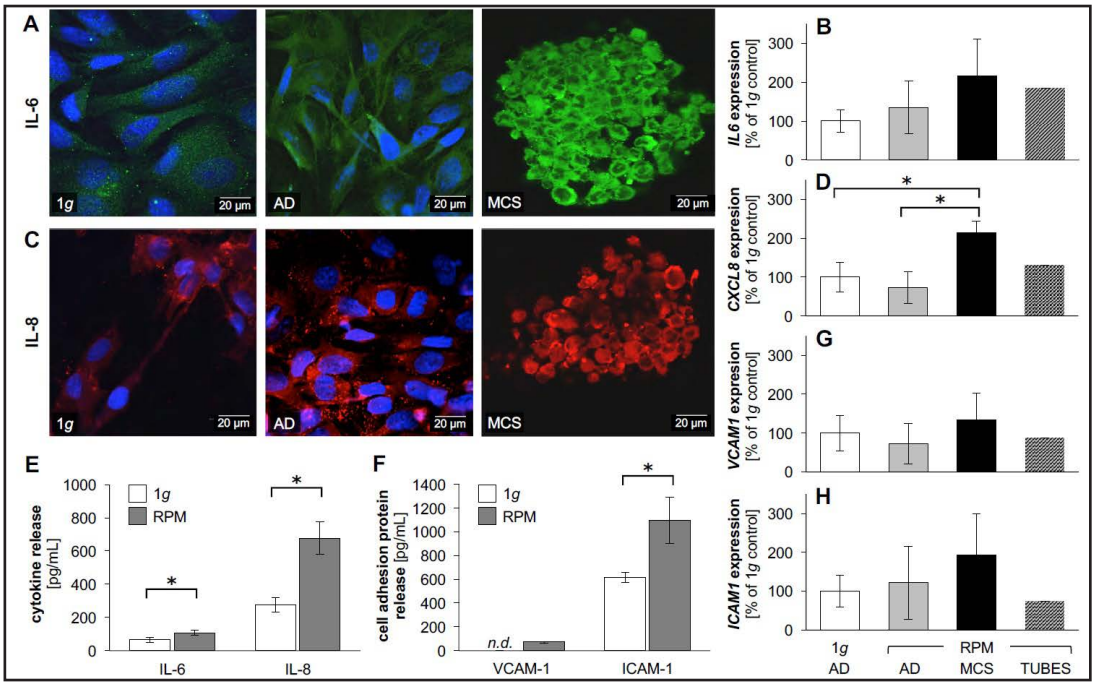

Fig. 5. Influence of RPM-exposure on interleukins and cell adhesion molecules: Quantitative alterations of protein content and gene expression of IL-6 and IL-8 after 35 d. IL-6. Immunofluorescence images of 1*g*-control cells, RPM-AD and RPM-MCS (A). Expression of *IL6* (B). IL-8. Immunofluorescence images of 1*g*-control cells, RPM-AD and RPM-MCS (C). Expression of *CXCL8* (D). Release of interleukins IL-6 and IL-8 (E). Release of the cell adhesion molecules VCAM-1 and ICAM-1 (F). Expression of *VCAM1* (G) and *ICAM1* (H). *p<0.05. Scale bars: 20 µm. n.d.: not detectable.

We also could detect an enhanced vascular cell adhesion molecule 1 (VCAM-1) and intercellular adhesion molecule 1 (ICAM-1) secretion after 35 d on the RPM (Fig. 5F), whereas the gene expressions of both cell adhesion molecules (*VCAM1* and *ICAM1*) were not significantly altered (Fig. 5G and 5H).

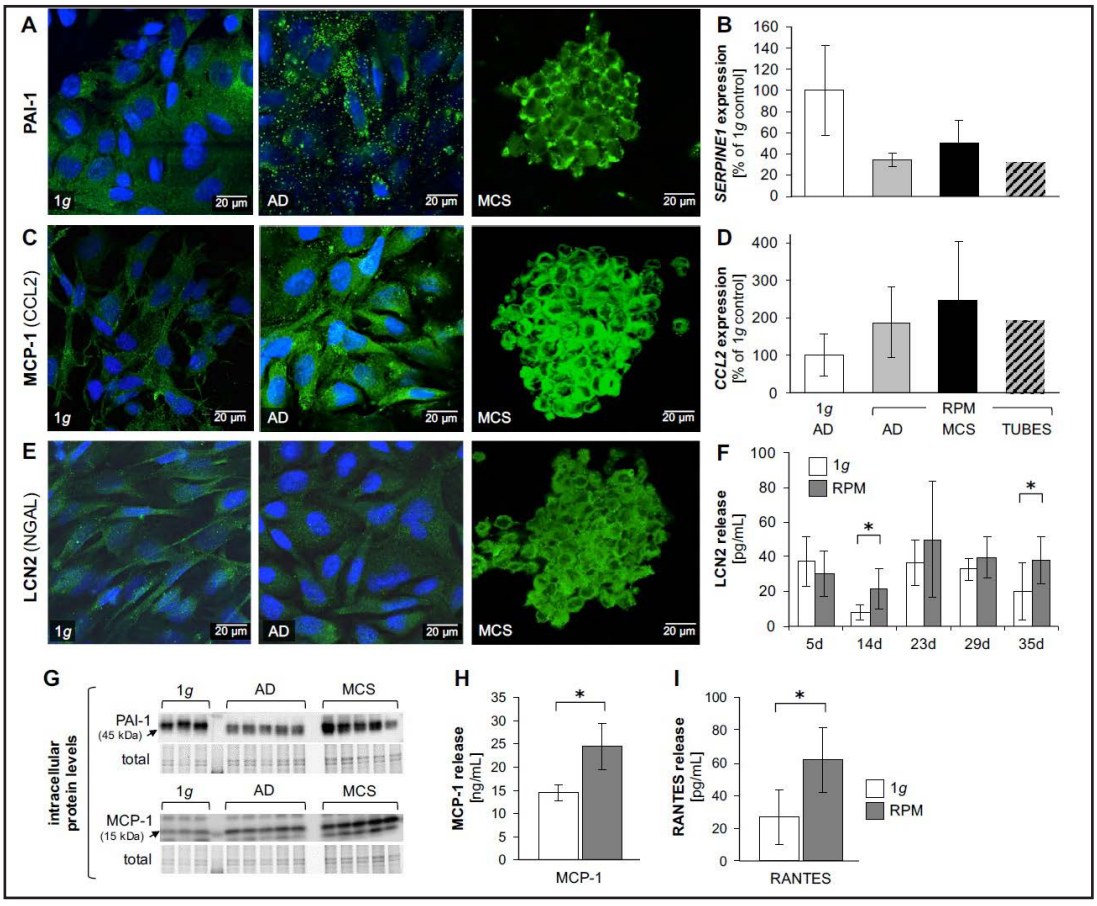

Fig. 6. Influence of RPM-exposure on soluble factors: Quantitative alterations of protein content and gene expression of PAI-1, MCP-1 (CCL2), and LCN2 (NGAL) after 35 d. PAI-1. Immunofluorescence images of 1*g*-control cells, RPM-AD and RPM-MCS (A). Expression of *SERPINE1* (B). MCP-1. Immunofluorescence images of 1*g*-control cells, RPM-AD and RPM-MCS after 35d (C). Expression of *CCL2* (D). LCN2. Immunofluorescence images of 1*g*-control cells, RPM-AD and RPM-MCS (E). Time course of LCN2 release (F). Intracellular levels of PAI-1 and MCP-1 determined via Western Blot (G) Release of MCP-1 (H) and RANTES (I). *p<0.05. Scale bars: 20 µm.

Selected factors involved in angiogenesis

Plasminogen activator inhibitor-1 (PAI-1) is also known as SERPINE1 and a risk factor for atherosclerosis and thrombosis. The immunofluorescence of PAI-1 revealed a concentration of the protein at the cellular membranes in MCS, possibly in connection with extracellular uPAR (Fig. 6A). PAI-1 is equally distributed in the cytoplasm of RPM-AD cells (Fig. 6A). The amount of the cellular protein is unchanged in all groups. *SERPINE1* mRNA levels were not changed in all groups (Fig. 6B). Western blotting revealed a slightly elevated amount of the PAI-1 protein in MCS compared to AD and 1*g*-cells (Fig. 6G).

IFS visualized an accumulation of monocyte chemoattractant protein 1 (MCP1, CCL2) protein in MCS (Fig. 6C). The release of MCP-1 protein was clearly increased in AD cells and MCS compared with 1*g*-samples (Fig. 6H). qPCR to measure the *CCL2* gene expression showed a tendency to an elevation in AD and MCS (Fig. 6D). A similar finding was seen in the Western Blot analysis (Fig. 6G).

The chemokine (C-C motif) ligand 5 (also CCL5) is also known as RANTES (regulated on activation, normal T cell expressed and secreted) [33]. It is of interest that the RANTES/CCL5-activity seems to be related to the *in vitro* promotion of endothelial cell migration, spreading and neo-vessel formation [33]. RANTES/CCL5-mediated angiogenesis depends

at least partly on VEGF secretion by ECs [33]. Here we could show that RANTES was clearly elevated in RPM-samples at day 35 compared to 1*g*-samples (Fig. 6I).

Neutrophil gelatinase-associated lipocalin (NGAL or LCN2) is detectable in activated neutrophils, kidney tubule cells, tumor cells, macrophages, vascular smooth muscle cells and endothelial cells. Recent studies have suggested that NGAL could also have pathophysiological importance in cardiovascular diseases [34]. We investigated NGAL by TRIFMA and found that its release in the supernatant is significantly elevated in RPM-samples at day 14 and day 35 (Fig. 6F). An accumulated NGAL in MCS was also detected by IFS (Fig. 6E).

Soluble factors released in the culture supernatant by the ECs

Concentrations of selected cytokines within 1*g* and RPM culture supernatants were determined by MAP analysis in order to measure the secretion behavior of the ECs. Table 3 shows all soluble factors of the InflammationMAP® v. 1.0, which were detectable.

C-reactive protein (CRP), eotaxin-1, factor VII, fibrinogen, haptoglobin, interferon gamma (IFN-gamma), interleukin-1 alpha (IL-1α), interleukin-1 beta (IL-1β), interleukin-1 receptor antagonist (IL-1ra), interleukin-2 (IL-2), interleukin-3 (IL-3), interleukin-4 (IL-4), interleukin-5 (IL-5), interleukin-7 (IL-7), interleukin-10 (IL-10), interleukin-12 subunit p40 (IL-12p40), interleukin-12 subunit p70 (IL-12p70), interleukin-15 (IL-15), interleukin-17 (IL-17), interleukin-18 (IL-18), interleukin-23 (IL-23), macrophage inflammatory protein-1 alpha (MIP-1α), macrophage inflammatory protein-1 beta (MIP-1β), matrix metalloprotein-

Table 3. Proteins released by EA.hy926 cells after a 35-day exposure to the RPM. The data was generated by Multi-Analyte Profiling using the Human Inflammation MAP® v1.0. Values are given as mean ± SD; ***,** P <0.05 vs. 1*g*; LLOQ (Lower Limit of Quantitation, lowest concentration of an analyte in a sample that can be reliably detected). The values are determined as the mean of 5 (1*g* control) or 13 (RPM) blank readings. C-reactive Protein (CRP), eotaxin-1, factor VII, fibrinogen, haptoglobin, interferon gamma (IFN-gamma), interleukin-1 alpha (IL-1α), interleukin-1 beta (IL-1β), interleukin-1 receptor antagonist (IL-1ra), interleukin-2 (IL-2), interleukin-3 (IL-3), interleukin-4 (IL-4), interleukin-5 (IL-5), interleukin-7 (IL-7), interleukin-10 (IL-10), interleukin-12 subunit p40 (IL-12p40), interleukin-12 subunit p70 (IL-12p70), interleukin-15 (IL-15), interleukin-17 (IL-17), interleukin-18 (IL-18), interleukin-23 (IL-23), macrophage inflammatory protein-1 alpha (MIP-1α), macrophage inflammatory protein-1 beta (MIP-1β), matrix metalloproteinase-3 (MMP-3), matrix metalloproteinase-9 (MMP-9), stem cell factor (SCF), tumor necrosis factor alpha (TNF-α), tumor necrosis factor beta (TNF-β), and vitamin D-binding protein (VDBP) levels were below the LLOQ

Factors	1*g* control	RPM	LLOQ	Units
Alpha-1-Antitrypsin (AAT)	0.087 ± 0.014	0.246 ± 0.095	0.075	ng/mL
Alpha-2-Macroglobulin (A2Macro)	1.240 ± 0.152	1.423 ± 0.174	0.520	µg/mL
Beta-2-Microglobulin (B2M)	73.0 ± 33.6	124.1 ± 46.3	0.042	µg/mL
Brain-Derived Neurotrophic Factor (BDNF)	0.590 ± 0.090	0.671 ± 0.104	0.008	ng/mL
Complement C3 (C3)	0.076 ± 0.032	0.412 ± 0.095*	0.027	ng/mL
Ferritin (FRTN)	0.247 ± 0.144	0.425 ± 0.079*	0.034	ng/mL
Granulocyte-Macrophage Colony-Stimulating Factor (GM-CSF)	< 5.6	8.862 ± 2.047	5.6	pg/mL
Intercellular Adhesion Molecule 1 (ICAM-1)	0.617 ± 0.040	1.110 ± 0.194	0.570	ng/mL
Interleukin-6 (IL-6)	64.8 ± 14.4	108.2 ± 15.7*	0.580	pg/mL
Interleukin-8 (IL-8)	276.8 ± 44.5	678.5 ± 98.3*	1.600	pg/mL
Monocyte Chemotactic Protein 1 (MCP-1)	14.56 ± 1.71	24.49 ± 4.95*	0.022	ng/mL
T-Cell-Specific Protein RANTES (RANTES)	0.027 ± 0.017	0.062 ± 0.020*	0.001	ng/mL
Tissue Inhibitor of Metalloproteinases 1 (TIMP-1)	53.2 ± 22.7	59.5 ± 20.6	0.013	ng/mL
Tumor necrosis factor receptor 2 (TNFR2)	0.017 ± 0.001	0.032 ± 0.005*	0.010	pg/mL
Vascular Cell Adhesion Molecule-1 (VCAM-1)	< 0.062	0.072 ± 0.006	0.062	ng/mL
Vascular Endothelial Growth Factor (VEGF)	25.8 ± 5.63	55.8 ± 13.3*	8.800	pg/mL
von Willebrand Factor (vWF)	0.033 ± 0.017	0.019 ± 0.007	0.002	µg/mL

ase-3 (MMP-3), matrix metalloproteinase-9 (MMP-9), stem cell factor (SCF), tumor necrosis factor alpha (TNF-α), tumor necrosis factor beta (TNF-β), and vitamin D-binding protein (VDBP) levels were below the Lower Limit of Quantification (LLOQ).

Alpha$_2$-macroglobulin, beta$_2$-microglobulin, brain-derived neurotrophic factor (BDNF), tissue inhibitor of metalloproteinases 1 (TIMP-1), von Willebrand Factor (vWF) and intercellular adhesion molecule-1 (ICAM-1) were detectable in the supernatant, but not altered in RPM-samples compared with 1*g*.

Vascular Cell Adhesion Molecule-1 (VCAM-1), granulocyte-macrophage colony-stimulating factor (GM-CSF), was below the LLOQ in 1*g* samples but detectable in RPM-samples. Alpha$_1$-antitrypsin (SERPINA1), complement C3 (C3), ferritin (FRTN), and tumor necrosis factor receptor 2 (TNFR-2 were significantly elevated in RPM-samples (Table 3).

Pathway Analyses

In order to see whether the up- and down-regulations in gene expression and protein accumulation within the cells or in the cell supernatant described above were isolated processes or are linked within a network of mutual influences, we applied STRING. Overall, the analysis showed that besides the ferritin, all the components investigated were part of a network of interaction either at protein or at transcriptional level (Fig. 7). This is true for components, which were known from earlier studies to be involved in tube or MCS formation as well as for components detected by the current MAP analysis (Table 3; Fig. 3, 4, 5 and 6).

At a protein level indicated by blue, purple, and black lines, FN1, TGFB1, VEGF, TIMP-1, FLT1, KDR and PAI-1, which were known from earlier studies play central roles together with the newly detected vWF, SERPINA1, and CSF2. In addition, C3 and RANTES contribute to this network via IL-8 [35, 36].

IL-6 and IL-8 appear to be mainly interactive in this system on a transcriptional level (yellow lines, grey lines with green arrowhead). IL-8 can up-regulate *IL6* and *VEGFA* expression, while IL-6 exerts influence on VEGFA, VCAM-1, ICAM-1, TIMP-1 and CCL2 expression [37-39]. VEGFA is also regulated by BDNF, LCN2 and PAI-1, but has positive regulatory effects on *FN1* [40, 41].

Discussion

In this study, we cultured EA.hy926 cells on a RPM, which was constructed to simulate microgravity conditions on Earth. Randomizing the gravity vector by the RPM keeps human cells floating in the medium and allows to study aspects of annulling gravity. A part of the incubated cells detaches from the bottom of a culture flask and forms 3D aggregates like they are observed after spaceflights [2, 4, 5, 19]. Even though in contrast to a stay in space, sheer forces are produced on the RPM, multicellular spheroids and tubular structures are formed in both conditions [18-20].

After EA.hy926 cells remained viable during a 35-d RPM-exposure, we could study genes and proteins favoring the formation and existence of 3D structures *in vitro.* EA.hy926 cells are hybrid cells obtained by a fusion of HUVEC and A549 lung cancer cells [13] and differ in their protein content considerably from primary endothelial cells like microvascular ECs [42]. Regarding their tube formation behavior, they are very similar compared to primary ECs, but are more robust [2, 42]. Adherent EA.hy926 cells started to diverge after 12 h of incubation on the RPM [30], while 1*g*-cultures continued to grow as monolayers and exhibited overgrowth and a lower viability and had to be subcultured weekly during the experiment. Large amounts of 3D structures were formed after 5 days on the RPM [8, 9, 42]. They included MCS and convoluted TS and clusters not previously seen in similar short-term experiments (Fig. 2). These TS elongated and formed branches, but were maintained when imposing turbulent flow in the culture flask, indicating a high degree of structural integrity of the MCS and TS.

Mechanisms for spheroid and tube formation of ECs exposed to the RPM

The *in vitro* growth of TS resembles blood vessel growth, which is controlled by several growth factors (VEGF, fibroblast growth factor, TGF-β_1) and by cytokines, such as interleukins. VEGF signaling is involved in various processes of tube formation such as EC migration, proliferation, and differentiation [43-46].

After a 35-d RPM-exposure, VEGF was accumulated in MCS as determined by immunofluorescence (Fig. 4A), while the mRNAs of *VEGF*, *FLT1* and *FLK1* were not differentially expressed. This is in contrast to increased *VEGF* expression found in previous experiments of shorter durations [9, 10, 42]. This finding may be explained by the different sizes of the spheroids, which were collected after 35 days and their high amount of proteins. The signal for the synthesis of VEGF may have been released earlier and this process is already completed after 35 days. Still, a significantly increased amount of VEGF165 was observed in RPM culture supernatants as compared to 1*g*-cultures at different time points (Fig. 4C).

In contrast to VEGF, the impact of TGF-β_1 in angiogenesis is still unclear. TGF-β_1 signaling might be important for vascular morphogenesis and stability [47], as it seems to support VEGF expression, while the effect of interaction on a protein level is still unknown (Fig. 7, [48]). According to the literature TGF-β_1 can act as a promotor or as an inhibitor of angiogenesis *in vivo* and *in vitro* [49], depending on the experimental conditions. In our experiment, the amount of TGF-β_1 protein was constant in 1*g*, AD and RPM-samples after 35 days as measured by Western blot analysis. Immunofluorescence staining delivered a similar result. In addition, the gene expression of *TGFB1* was not altered. This indicates that the role of TGF-β_1 in spheroid and tube formation is more marginal.

Synthesis and maintenance of the ECM is important for the function of ECs. Here we measured the mRNA of collagen IV. The *COL4A1* gene expression was not altered in AD, MCS and TS cells after 35d. In addition, we focused on the ECM protein and cell adhesion molecule fibronectin, which plays an important role in wound healing and inflammation [21, 22]. Fibronectin is involved in migration, cell adhesion, differentiation processes and its expression is altered in various disorders such as diabetes, ischemia and reperfusion [50] as well as other cardiovascular disorders or cancers [50]. Anderson *et al* [51]. showed that an elevation in ECM synthesis in micropattern-elongated ECs is regulated by TGF-β_1 (see also Fig. 7), and that an elevated ECM might be important for the maintenance of a healthy endothelium *in vivo*. Its role in tissue engineering of TS might be more important in short-term studies. After a prolonged RPM-exposure, the measured increase in *FN1* mRNA and the accumulation of fibronectin may also play a key role in a healthy endothelium and relevant for the process of angiogenesis. We found a clear increase in fibronectin protein in MCS compared to μ*g*-AD cells and 1*g*-cells after 35 days. This is similar to previous findings at shorter durations [8, 10, 30]. Elevated fibronectin contributes to the activity of VEGF, and the combination of both proteins present at higher levels would likely contribute greatly to angiogenesis [52]. Furthermore, it is plausible that lower levels of fibronectin facilitate the detachment of cells from the monolayer, as fibronectin is involved in the adhesion cells to the culture flask. Earlier analyses with thyroid cancer cells expressing surface proteins that bind fibronectin, support the hypothesis concerning the role of fibronectin in 3D growth of human cells [53].

Enhanced amounts of IL-6 and IL-8 were detected in MCS and a significantly enhanced release of IL-6 and IL-8 was measured by MAP technology in RPM-cultures. This points to enhancement of IL-6 and IL-8 production under microgravity. Both cytokines play a role in wound repair and inflammation and increased amounts were secreted in the culture supernatant by the ECs. IL-6 is involved in angiogenesis and vascular remodeling [54]. IL-6 protein was elevated in the MCS. A similar result was detected for IL-8. In parallel, the *CXCL8* mRNA was significantly elevated in MCS compared to AD and 1*g*-cultures (Fig. 5D). In our system, both interleukins seem to exert their effects favoring angiogenesis via enhancement of expression of VCAM-1, ICAM-1 and VEGF165 (Fig. 7).

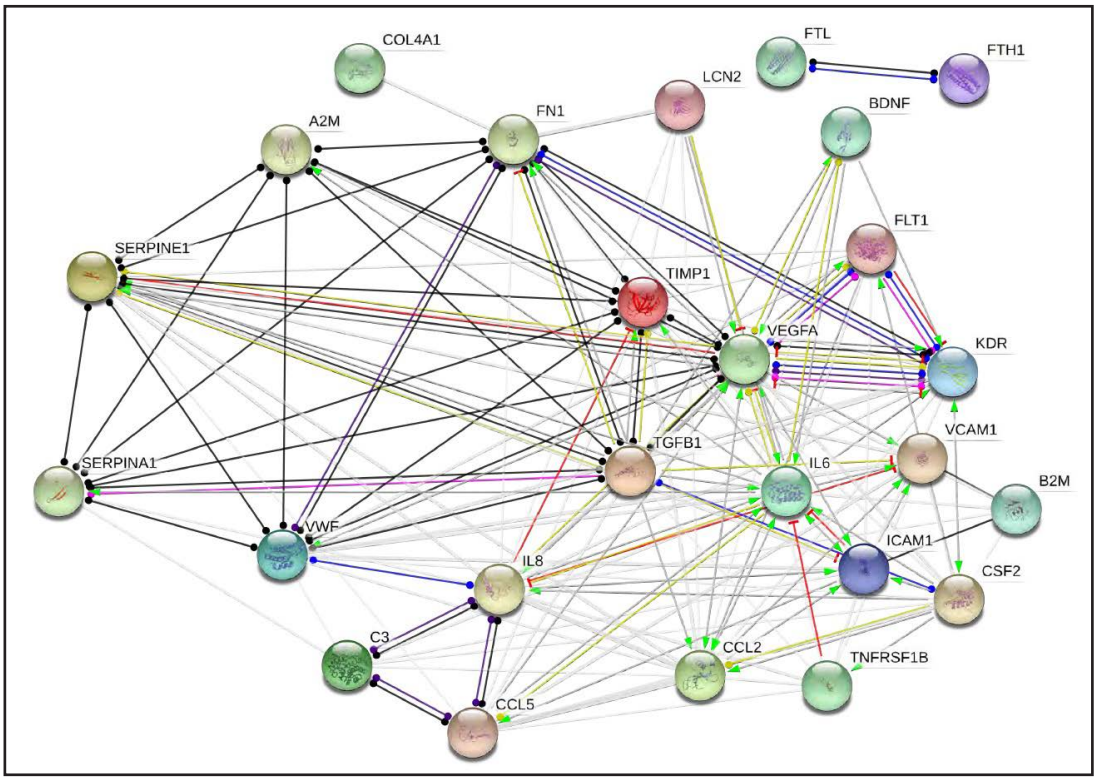

Fig. 7. STRING analysis of the proteins investigated in this study: FN1, VEGFA, MCP-1, TGF-β_1, PAI-1, IL-6, IL-8, COL4A1, FLK1, FLT1, VCAM-1, TNFR2, TIMP-1, ICAM-1, CCL2, A2M, B2M and LCN2 were used because earlier studies suggested their involvement in 3D structure formation. vWF, CCL5, C3, BDNF and SERPINA1 were detected in the current MAP analysis. The colors of the lines mean type of interaction: black line, undefined reactions, blue line, binding; purple line, posttranslational modification; red line, inhibition; yellow line, influence on expression; grey line with green arrow head, support of expression.

Multianalyte profiling also revealed an increase in the secretion of VCAM-1 in RPM-cultures, whereas VCAM-1 was not detectable in 1*g*-samples. In addition, the release of ICAM-1 was significantly elevated by long-term RPM-exposure of the ECs. Both adhesion molecules mediate the adhesion of several cell types such as lymphocytes, tumor cells and others to vascular endothelium [55]. In inflammation disorders the VCAM-1 expression is induced on the EC by cytokines or shear stress [56]. VCAM is detectable at the surface of the EC. Thereafter, the EC are activated to express adhesion molecules mediating leukocyte binding and to reveal a changed EC shape [56]. It has been shown that angiogenesis induced *in vivo* in rat cornea and dependent on IL-4 and IL-13, is mainly mediated through a soluble VCAM-1/α4 integrin pathway [57]. In addition, ICAM-1 is capable to induce angiogenesis and to increase the survival of microvessels [58]. Increased amounts of VCAM-1 and ICAM-1 in RPM-cultures might support 3D formation of ECs exposed to the RPM.

Plasminogen activator inhibitor-1 (PAI-1 or serpin E1) is normally known as the principal inhibitor of tissue plasminogen activator (tPA) and urokinase (uPA). PAI-1 is mainly produced by ECs, but is also secreted by other cells, e.g. thyroid cancer cells [59]. PAI-1 is involved in cancer angiogenesis, metastasis and promotes angiogenesis by stimulating EC migration toward fibronectin [60]. It also plays a role during retinal angiogenesis [61] and has been demonstrated to support angiogenesis in cancer. Geis *et al.* [62] showed that the HIF-2α-dependent PAI-1 induction contributes to angiogenesis in hepatocellular carcinoma. PAI-1 was already examined in microgravity studies and was reduced after a short-term RPM-exposure of ECs [15]. This is in line with our results showing a reduction in the AD cells after 35 days. A decrease in PAI-1 may initiate an increase in active plasmin, which

may be important for ECM remodeling and 3D formation. In addition, the inhibitory effect on VEGFA may be attenuated (see Fig. 7 red line, [40]). In clinical settings, increased plasma levels of plasmin are associated with an increased risk of atherosclerosis and myocardial infarction [63]. Moreover, in thyroid cancer cells exposed for 24 h to the RPM, the *PAI1* mRNA was reduced in the presence of elevated *VEGF*, while the *TGFB1* mRNA was not altered. In an earlier study, we had shown that increased plasminogen is relevant for the inhibition of spheroid formation [64]. These data support the thesis that downregulation of PAI-1 could help to form spheroids [65], because soluble PAI-1 is linked to inflammation, endothelium dysfunction and cardiovascular disease [66] and cancer metastasis.

Monocyte chemoattractant protein-1 (MCP-1)/CCL2 is synthesized and secreted by various cell types. ECs express functional CCR2, which is important for endothelial wound repair and inflammatory reactions. Consistent with previous research of shorter durations, we found MCP-1 protein to be elevated in both AD cells and MCS as determined by immunofluorescence and detected a similar trend in the Western blot analyses. The *MCP1* (*CCL2*) gene expression was not significantly changed, but MCS revealed a tendency of an increase in CCL2. Its role in the formation of spheroids or tubes remains to be investigated in future studies as a stimulatory effect on expression of VEGFA, ICAM-1 and VCAM-1 is suggested by the STRING analysis.

Additional soluble factors released in the supernatant

As detected by MAP technology several proteins were released by the EC in the culture supernatant after 35 days (Table 3). An increased secretion was measured for alpha-1-antitrypsin, GM-CSF, T-cell-specific protein RANTES, complement C3, ferritin, tumor necrosis factor receptor 2 in RPM-samples. In contrast, the release of alpha-2-macroglobulin, beta-2-microglobulin, brain-derived neurotrophic factor, tissue inhibitor of metalloproteinases 1 and von Willebrand Factor in ECs remained unchanged, when the cells were cultured for 35 days on the RPM. All of these factors are members of the network shown in Fig. 7. Although unknown so far in detail, SERPINA1 and vWF appear to play a significant role.

In addition, we measured NGAL by TRIFMA. Recent publications showed that NGAL, a biomarker for kidney disease has also a pathophysiological importance in cardiovascular diseases. It has negative regulatory influence on *VEGFA* transcription (Fig. 7 red cross bar, [67]). We had investigated the time course of NGAL secretion and found an increase with significance in RPM culture supernatants after 35 d (Fig. 6F). Furthermore, NGAL had been detected in different cancer types [25, 31]. Its role in 3D growth of ECs has to be studied in more detail in the future.

Conclusion

A long-term exposure of EA.hy926 cells to the RPM changed the growth behavior of the cells. Like observed on primary microvascular endothelial cells, three different phenotypes appeared: adherently growing cells at the bottom of the culture flasks, multicellular spheroids and 3D tubular structures, both in suspension in the culture supernatant. Consistent with earlier data [8, 9] and observations made during the ESA-SPHEROIDS space mission to the ISS [2], the MCS developed during the first two weeks [2]. Using EA.hy926 cells, we could expand this period and demonstrate that VEGF, IL-6, IL-8, PAI-1, ICAM-1 and VCAM-1 are interesting proteins involved in the changed growth behavior and the development of the three phenotypes. Especially MCP-1 and NGAL are interesting targets for future experiments.

Acknowledgements

The authors would like to thank the German Space Agency (DLR; (DG) BMWi project 50WB1524), and Aarhus University, Denmark. The funders had no role in study design, data collection and analysis, decision to publish, or preparation of the manuscript.

D.G. and N.E.M. designed the experiments. A.D., and J.S. executed the experiments and collected the material. A.D. and N.E.M. performed western blot analyses. M.K., A.D. and N.E.M. performed qPCR analyses. J.B. performed the pathway analyses. D.G., J.B., N.E.M. and M.K. wrote the manuscript. M.I. contributed reagents, materials and analysis tools. All authors reviewed the manuscript.

Disclosure Statement

Competing financial interests: The authors declare no competing financial interests.

References

1 Hallgren E, Migeotte P-F, Kornilova L, Delière Q, Fransen E, Glukhikh D, Moore ST, Clément G, Diedrich A, MacDougall H, Wuyts FL: Dysfunctional vestibular system causes a blood pressure drop in astronauts returning from space. Sci Rep 2015;5:17627.

2 Pietsch J, Gass S, Nebuloni S, Echegoyen D, Riwaldt S, Baake C, Bauer J, Corydon TJ, Egli M, Infanger M, Grimm D: Three-dimensional growth of human endothelial cells in an automated cell culture experiment container during the SpaceX CRS-8 ISS space mission - The SPHEROIDS project. Biomaterials 2017;124:126-156.

3 Versari S, Longinotti G, Barenghi L, Maier JA, Bradamante S: The challenging environment on board the International Space Station affects endothelial cell function by triggering oxidative stress through thioredoxin interacting protein overexpression: the ESA-SPHINX experiment. Faseb j 2013;27:4466-4475.

4 Aleshcheva G, Bauer J, Hemmersbach R, Slumstrup L, Wehland M, Infanger M, Grimm D: Scaffold-free Tissue Formation Under Real and Simulated Microgravity Conditions. Basic Clin Pharmacol Toxicol 2016;119:S26-33.

5 Grimm D, Wehland M, Pietsch J, Aleshcheva G, Wise P, van Loon J, Ulbrich C, Magnusson NE, Infanger M, Bauer J: Growing tissues in real and simulated microgravity: new methods for tissue engineering. Tissue Eng Part B Rev 2014;20:555-566.

6 Janmaleki M, Pachenari M, Seyedpour SM, Shahghadami R, Sanati-Nezhad A: Impact of Simulated Microgravity on Cytoskeleton and Viscoelastic Properties of Endothelial Cell. Sci Rep 2016;6:32418.

7 Shi F, Wang YC, Hu ZB, Xu HY, Sun J, Gao Y, Li XT, Yang CB, Xie C, Li CF, Zhang S, Zhao JD, Cao XS, Sun XQ: Simulated Microgravity Promotes Angiogenesis through RhoA-Dependent Rearrangement of the Actin Cytoskeleton. Cell Physiol Biochem 2017;41:227-238.

8 Grimm D, Infanger M, Westphal K, Ulbrich C, Pietsch J, Kossmehl P, Vadrucci S, Baatout S, Flick B, Paul M, Bauer J: A delayed type of three-dimensional growth of human endothelial cells under simulated weightlessness. Tissue Eng Part A 2009;15:2267-2275.

9 Grimm D, Bauer J, Ulbrich C, Westphal K, Wehland M, Infanger M, Aleshcheva G, Pietsch J, Ghardi M, Beck M, El-Saghire H, de Saint-Georges L, Baatout S: Different responsiveness of endothelial cells to vascular endothelial growth factor and basic fibroblast growth factor added to culture media under gravity and simulated microgravity. Tissue Eng Part A 2010;16:1559-1573.

10 Grosse J, Wehland M, Pietsch J, Ma X, Ulbrich C, Schulz H, Saar K, Hubner N, Hauslage J, Hemmersbach R, Braun M, van Loon J, Vagt N, Infanger M, Eilles C, Egli M, Richter P, Baltz T, Einspanier R, Sharbati S, Grimm D: Short-term weightlessness produced by parabolic flight maneuvers altered gene expression patterns in human endothelial cells. Faseb j 2012;26:639-655.

11 Infanger M, Ulbrich C, Baatout S, Wehland M, Kreutz R, Bauer J, Grosse J, Vadrucci S, Cogoli A, Derradji H, Neefs M, Kusters S, Spain M, Paul M, Grimm D: Modeled gravitational unloading induced downregulation of endothelin-1 in human endothelial cells. J Cell Biochem 2007;101:1439-1455.

12 Häder DP, Braun M, Grimm D, Hemmersbach R: Gravireceptors in eukaryotes-a comparison of case studies on the cellular level. NPJ Microgravity 2017;3:13.

13 Edgell CJ, McDonald CC, Graham JB: Permanent cell line expressing human factor VIII-related antigen established by hybridization. Proc Natl Acad Sci U S A 1983;80:3734-3737.

14 Borst AG, van Loon JJWA: Technology and Developments for the Random Positioning Machine, RPM. Microgravity Sci Technol 2008;21:287.
15 Ma X, Wehland M, Schulz H, Saar K, Hubner N, Infanger M, Bauer J, Grimm D: Genomic approach to identify factors that drive the formation of three-dimensional structures by EA.hy926 endothelial cells. PLoS One 2013;8:e64402.
16 Ulbrich C, Westphal K, Baatout S, Wehland M, Bauer J, Flick B, Infanger M, Kreutz R, Vadrucci S, Egli M, Cogoli A, Derradji H, Pietsch J, Paul M, Grimm D: Effects of basic fibroblast growth factor on endothelial cells under conditions of simulated microgravity. J Cell Biochem 2008;104:1324-1341.
17 Ulbrich C, Westphal K, Pietsch J, Winkler HD, Leder A, Bauer J, Kossmehl P, Grosse J, Schoenberger J, Infanger M, Egli M, Grimm D: Characterization of human chondrocytes exposed to simulated microgravity. Cell Physiol Biochem 2010;25:551-560.
18 Wuest SL, Richard S, Kopp S, Grimm D, Egli M: Simulated microgravity: critical review on the use of random positioning machines for mammalian cell culture. Biomed Res Int 2015;2015:971474.
19 Warnke E, Pietsch J, Wehland M, Bauer J, Infanger M, Gorog M, Hemmersbach R, Braun M, Ma X, Sahana J, Grimm D: Spheroid formation of human thyroid cancer cells under simulated microgravity: a possible role of CTGF and CAV1. Cell Commun Signal 2014;12:32.
20 Svejgaard B, Wehland M, Ma X, Kopp S, Sahana J, Warnke E, Aleshcheva G, Hemmersbach R, Hauslage J, Grosse J, Bauer J, Corydon TJ, Islam T, Infanger M, Grimm D: Common Effects on Cancer Cells Exerted by a Random Positioning Machine and a 2D Clinostat. PLoS One 2015;10:e0135157.
21 Infanger M, Grosse J, Westphal K, Leder A, Ulbrich C, Paul M, Grimm D: Vascular endothelial growth factor induces extracellular matrix proteins and osteopontin in the umbilical artery. Ann Vasc Surg 2008;22:273-284.
22 Infanger M, Shakibaei M, Kossmehl P, Hollenberg SM, Grosse J, Faramarzi S, Schulze-Tanzil G, Paul M, Grimm D: Intraluminal application of vascular endothelial growth factor enhances healing of microvascular anastomosis in a rat model. J Vasc Res 2005;42:202-213.
23 Pietsch J, Kussian R, Sickmann A, Bauer J, Weber G, Nissum M, Westphal K, Egli M, Grosse J, Schonberger J, Wildgruber R, Infanger M, Grimm D: Application of free-flow IEF to identify protein candidates changing under microgravity conditions. Proteomics 2010;10:904-913.
24 Grosse J, Warnke E, Pohl F, Magnusson NE, Wehland M, Infanger M, Eilles C, Grimm D: Impact of sunitinib on human thyroid cancer cells. Cell Physiol Biochem 2013;32:154-170.
25 Kopp S, Warnke E, Wehland M, Aleshcheva G, Magnusson NE, Hemmersbach R, Corydon TJ, Bauer J, Infanger M, Grimm D: Mechanisms of three-dimensional growth of thyroid cells during long-term simulated microgravity. Sci Rep 2015;5:16691.
26 Magnusson NE, Hornum M, Jorgensen KA, Hansen JM, Bistrup C, Feldt-Rasmussen B, Flyvbjerg A: Plasma neutrophil gelatinase associated lipocalin (NGAL) is associated with kidney function in uraemic patients before and after kidney transplantation. BMC Nephrol 2012;13:8.
27 Rothermund L, Kreutz R, Kossmehl P, Fredersdorf S, Shakibaei M, Schulze-Tanzil G, Paul M, Grimm D: Early onset of chondroitin sulfate and osteopontin expression in angiotensin II-dependent left ventricular hypertrophy. Am J Hypertens 2002;15:644-652.
28 Snel B, Lehmann G, Bork P, Huynen MA: STRING: a web-server to retrieve and display the repeatedly occurring neighbourhood of a gene. Nucleic Acids Res 2000;28:3442-3444.
29 Pietsch J, Riwaldt S, Bauer J, Sickmann A, Weber G, Grosse J, Infanger M, Eilles C, Grimm D: Interaction of proteins identified in human thyroid cells. Int J Mol Sci 2013;14:1164-1178.
30 Infanger M, Kossmehl P, Shakibaei M, Baatout S, Witzing A, Grosse J, Bauer J, Cogoli A, Faramarzi S, Derradji H, Neefs M, Paul M, Grimm D: Induction of three-dimensional assembly and increase in apoptosis of human endothelial cells by simulated microgravity: impact of vascular endothelial growth factor. Apoptosis 2006;11:749-764.
31 Kopp S, Slumstrup L, Corydon TJ, Sahana J, Aleshcheva G, Islam T, Magnusson NE, Wehland M, Bauer J, Infanger M, Grimm D: Identifications of novel mechanisms in breast cancer cells involving duct-like multicellular spheroid formation after exposure to the Random Positioning Machine. Sci Rep 2016;6:26887.
32 Warnke E, Pietsch J, Kopp S, Bauer J, Sahana J, Wehland M, Krüger M, Hemmersbach R, Infanger M, Lutzenberg R, Grimm D: Cytokine Release and Focal Adhesion Proteins in Normal Thyroid Cells Cultured on the Random Positioning Machine. Cell Physiol Biochem 2017;43:257-270.

33 Suffee N, Hlawaty H, Meddahi-Pelle A, Maillard L, Louedec L, Haddad O, Martin L, Laguillier C, Richard B, Oudar O, Letourneur D, Charnaux N, Sutton A: RANTES/CCL5-induced pro-angiogenic effects depend on CCR1, CCR5 and glycosaminoglycans. Angiogenesis 2012;15:727-744.
34 Eilenberg W, Stojkovic S, Piechota-Polanczyk A, Kaun C, Rauscher S, Groger M, Klinger M, Wojta J, Neumayer C, Huk I, Demyanets S: Neutrophil Gelatinase-Associated Lipocalin (NGAL) is Associated with Symptomatic Carotid Atherosclerosis and Drives Pro-inflammatory State *In vitro*. Eur J Vasc Endovasc Surg 2016;51:623-631.
35 Lappegard KT, Bergseth G, Riesenfeld J, Pharo A, Magotti P, Lambris JD, Mollnes TE: The artificial surface-induced whole blood inflammatory reaction revealed by increases in a series of chemokines and growth factors is largely complement dependent. J Biomed Mater Res A 2008;87:129-135.
36 Lee TH, Avraham H, Lee SH, Avraham S: Vascular endothelial growth factor modulates neutrophil transendothelial migration via up-regulation of interleukin-8 in human brain microvascular endothelial cells. J Biol Chem 2002;277:10445-10451.
37 Heinrich PC, Behrmann I, Haan S, Hermanns HM, Muller-Newen G, Schaper F: Principles of interleukin (IL)-6-type cytokine signalling and its regulation. Biochem J 2003;374:1-20.
38 Xie K: Interleukin-8 and human cancer biology. Cytokine Growth Factor Rev 2001;12:375-391.
39 Zhang GJ, Crist SA, McKerrow AK, Xu Y, Ladehoff DC, See WA: Autocrine IL-6 production by human transitional carcinoma cells upregulates expression of the alpha5beta1 firbonectin receptor. J Urol 2000;163:1553-1559.
40 Wu J, Strawn TL, Luo M, Wang L, Li R, Ren M, Xia J, Zhang Z, Ma W, Luo T, Lawrence DA, Fay WP: Plasminogen activator inhibitor-1 inhibits angiogenic signaling by uncoupling vascular endothelial growth factor receptor-2-alphaVbeta3 integrin cross talk. Arterioscler Thromb Vasc Biol 2015;35:111-120.
41 Wu T, Zhang B, Ye F, Xiao Z: A potential role for caveolin-1 in VEGF-induced fibronectin upregulation in mesangial cells: involvement of VEGFR2 and Src. Am J Physiol Renal Physiol 2013;304:F820-830.
42 Ma X, Sickmann A, Pietsch J, Wildgruber R, Weber G, Infanger M, Bauer J, Grimm D: Proteomic differences between microvascular endothelial cells and the EA.hy926 cell line forming three-dimensional structures. Proteomics 2014;14:689-698.
43 Ferrara N, Gerber HP, LeCouter J: The biology of VEGF and its receptors. Nat Med 2003;9:669-676.
44 Kristensen TB, KnuTSon ML, Wehland M, Laursen BE, Grimm D, Warnke E, Magnusson NE: Anti-vascular endothelial growth factor therapy in breast cancer. Int J Mol Sci 2014;15:23024-23041.
45 Tammela T, Enholm B, Alitalo K, Paavonen K: The biology of vascular endothelial growth factors. Cardiovasc Res 2005;65:550-563.
46 Wehland M, Bauer J, Magnusson NE, Infanger M, Grimm D: Biomarkers for anti-angiogenic therapy in cancer. Int J Mol Sci 2013;14:9338-9364.
47 Pardali E, ten Dijke P: Transforming growth factor-beta signaling and tumor angiogenesis. Front Biosci (Landmark Ed) 2009;14:4848-4861.
48 Breier G, Blum S, Peli J, Groot M, Wild C, Risau W, Reichmann E: Transforming growth factor-beta and Ras regulate the VEGF/VEGF-receptor system during tumor angiogenesis. Int J Cancer 2002;97:142-148.
49 Goumans MJ, Liu Z, ten Dijke P: TGF-beta signaling in vascular biology and dysfunction. Cell Res 2009;19:116-127.
50 Kossmehl P, Schonberger J, Shakibaei M, Faramarzi S, Kurth E, Habighorst B, von Bauer R, Wehland M, Kreutz R, Infanger M, Schulze-Tanzil G, Paul M, Grimm D: Increase of fibronectin and osteopontin in porcine hearts following ischemia and reperfusion. J Mol Med (Berl) 2005;83:626-637.
51 Anderson DE, Hinds MT: Extracellular matrix production and regulation in micropatterned endothelial cells. Biochem Biophys Res Commun 2012;427:159-164.
52 Wijelath ES, Rahman S, Namekata M, Murray J, Nishimura T, Mostafavi-Pour Z, Patel Y, Suda Y, Humphries MJ, Sobel M: Heparin-II domain of fibronectin is a vascular endothelial growth factor-binding domain: enhancement of VEGF biological activity by a singular growth factor/matrix protein synergism. Circ Res 2006;99:853-860.
53 Pietsch J, Sickmann A, Weber G, Bauer J, Egli M, Wildgruber R, Infanger M, Grimm D: A proteomic approach to analysing spheroid formation of two human thyroid cell lines cultured on a random positioning machine. Proteomics 2011;11:2095-2104.

54 Yao JS, Zhai W, Fan Y, Lawton MT, Barbaro NM, Young WL, Yang GY: Interleukin-6 upregulates expression of KDR and stimulates proliferation of human cerebrovascular smooth muscle cells. J Cereb Blood Flow Metab 2007;27:510-520.
55 Eibl RH, Benoit M: Molecular resolution of cell adhesion forces. IEE Proc Nanobiotechnol 2004;151:128-132.
56 Cook-Mills JM, Marchese ME, Abdala-Valencia H: Vascular cell adhesion molecule-1 expression and signaling during disease: regulation by reactive oxygen species and antioxidants. Antioxid Redox Signal 2011;15:1607-1638.
57 Fukushi J, Ono M, Morikawa W, Iwamoto Y, Kuwano M: The activity of soluble VCAM-1 in angiogenesis stimulated by IL-4 and IL-13. J Immunol 2000;165:2818-2823.
58 Deng C, Zhang D, Shan S, Wu J, Yang H, Yu Y: Angiogenic effect of intercellular adhesion molecule-1. J Huazhong Univ Sci Technolog Med Sci 2007;27:9-12.
59 Riwaldt S, Bauer J, Pietsch J, Braun M, Segerer J, Schwarzwalder A, Corydon TJ, Infanger M, Grimm D: The Importance of Caveolin-1 as Key-Regulator of Three-Dimensional Growth in Thyroid Cancer Cells Cultured under Real and Simulated Microgravity Conditions. Int J Mol Sci 2015;16:28296-28310.
60 Isogai C, Laug WE, Shimada H, Declerck PJ, Stins MF, Durden DL, Erdreich-Epstein A, DeClerck YA: Plasminogen activator inhibitor-1 promotes angiogenesis by stimulating endothelial cell migration toward fibronectin. Cancer Res 2001;61:5587-5594.
61 Basu A, Menicucci G, Maestas J, Das A, McGuire P: Plasminogen activator inhibitor-1 (PAI-1) facilitates retinal angiogenesis in a model of oxygen-induced retinopathy. Invest Ophthalmol Vis Sci 2009;50:4974-4981.
62 Geis T, Doring C, Popp R, Grossmann N, Fleming I, Hansmann ML, Dehne N, Brune B: HIF-2alpha-dependent PAI-1 induction contributes to angiogenesis in hepatocellular carcinoma. Exp Cell Res 2015;331:46-57.
63 Ploplis VA: Effects of altered plasminogen activator inhibitor-1 expression on cardiovascular disease. Curr Drug Targets 2011;12:1782-1789.
64 Riwaldt S, Pietsch J, Sickmann A, Bauer J, Braun M, Segerer J, Schwarzwalder A, Aleshcheva G, Corydon TJ, Infanger M, Grimm D: Identification of proteins involved in inhibition of spheroid formation under microgravity. Proteomics 2015;15:2945-2952.
65 Liekens S, De Clercq E, Neyts J: Angiogenesis: regulators and clinical applications. Biochem Pharmacol 2001;61:253-270.
66 Verma S, Buchanan MR, Anderson TJ: Endothelial function testing as a biomarker of vascular disease. Circulation 2003;108:2054-2059.
67 Tong Z, Kunnumakkara AB, Wang H, Matsuo Y, Diagaradjane P, Harikumar KB, Ramachandran V, Sung B, Chakraborty A, Bresalier RS, Logsdon C, Aggarwal BB, Krishnan S, Guha S: Neutrophil gelatinase-associated lipocalin: a novel suppressor of invasion and angiogenesis in pancreatic cancer. Cancer Res 2008;68:6100-6108.